AD-A182 963 PHOTOLUMINESCENT PROPERTIES OF P-GAAS ELECTRODES RELATED TO THE 'PHOTOCUR..(U) WISCONSIN UNIV-MADISON DEPT OF CHEMISTRY P B JOHNSON ET AL. 08 JUL 87 UNCLASSIFIED UWIS/DC/TR-87/4 N00014-85-K-0631 F/G 9/5 NL

1/1

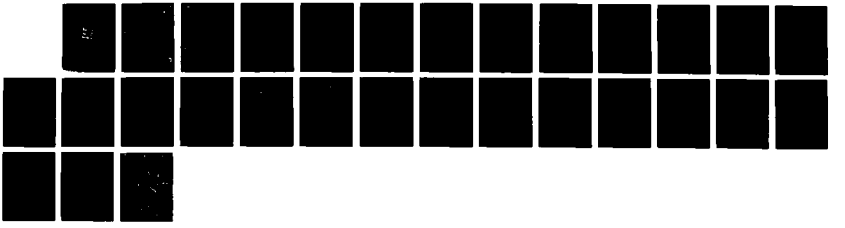

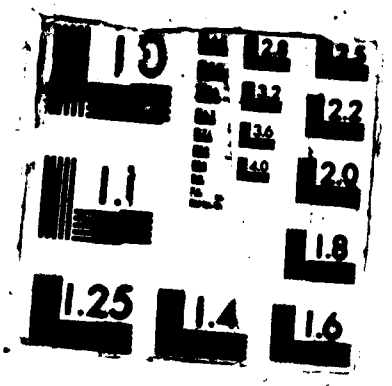
1.0
2.2
1.1
2.0
1.8
1.25
1.4
1.6

OFFICE OF NAVAL RESEARCH

Contract N00014-85-K-0631

R&T Code 4134003

Technical Report No. UWIS/DC/TR-87/4

Photoluminescent Properties of p-GaAs Electrodes Related to the "Photocurrent Anomaly": Determination of Surface Electron-Capture Velocities and Depletion Widths in Photoelectrochemical Cells

by

Phelps B. Johnson, Christopher S. McMillan, Arthur B. Ellis,* and William S. Hobson

Prepared for Publication in the

Journal of Applied Physics

University of Wisconsin
Department of Chemistry
Madison, Wisconsin 53706

July 8, 1987

*To whom all correspondence should be addressed

Unclassified
SECURITY CLASSIFICATION OF THIS PAGE

A182963

REPORT DOCUMENTATION PAGE

1a. REPORT SECURITY CLASSIFICATION NA	1b. RESTRICTIVE MARKINGS NA
2a. SECURITY CLASSIFICATION AUTHORITY NA	3. DISTRIBUTION / AVAILABILITY OF REPORT Distribution Unlimited; Approved for Public Release
2b. DECLASSIFICATION / DOWNGRADING SCHEDULE NA	
4. PERFORMING ORGANIZATION REPORT NUMBER(S) UWIS/DC/TR-87/4	5. MONITORING ORGANIZATION REPORT NUMBER(S) NA
6a. NAME OF PERFORMING ORGANIZATION Chemistry Department University of Wisconsin-Madison 6b. OFFICE SYMBOL (If applicable)	7a. NAME OF MONITORING ORGANIZATION ONR
6c. ADDRESS (City, State, and ZIP Code) 1101 University Avenue Madison, WI 53706	7b. ADDRESS (City, State, and ZIP Code) 800 N. Quincy St. Arlington, VA 22217
8a. NAME OF FUNDING / SPONSORING ORGANIZATION 8b. OFFICE SYMBOL (If applicable) NA	9. PROCUREMENT INSTRUMENT IDENTIFICATION NUMBER Contract N00014-85-K-0631
8c. ADDRESS (City, State, and ZIP Code)	10. SOURCE OF FUNDING NUMBERS PROGRAM ELEMENT NO. / PROJECT NO. / TASK NO. R&T Code 4134003 / WORK UNIT ACCESSION NO

11. TITLE (Include Security Classification)
Photoluminescent Properties of p-GaAs Electrodes Related to the "Photocurrent Anomaly": Determination of Surface Electron-Capture Velocities and Depletion Widths in Photoelectrochemical Cells

12. PERSONAL AUTHOR(S)
Phelps B. Johnson, Christopher S. McMillan, Arthur B. Ellis, and William S. Hobson

13a. TYPE OF REPORT	13b. TIME COVERED	14. DATE OF REPORT (Year, Month, Day)	15. PAGE COUNT
Technical	FROM _____ TO _____	6/20/87	29

16. SUPPLEMENTARY NOTATION
Prepared for publication in the Journal of Applied Physics

17. COSATI CODES		
FIELD	GROUP	SUB-GROUP

18. SUBJECT TERMS (Continue on reverse if necessary and identify by block number)
~~p-GaAs~~; photoluminescence; dead layer model; depletion width, surface electron capture velocity; photoelectrochemical cells, Gallium Arsenides,

19. ABSTRACT (Continue on reverse if necessary and identify by block number)

Steady-state photoluminescence (PL) measurements have been used to determine depletion widths W and surface electron-capture velocities S for p-GaAs electrodes in aqueous acidic electrolytes. Electrodes subjected to slow cycling of applied potential (10 mV/s) exhibit a hysteresis in PL intensity in the "photocurrent anomaly" (PA) potential regime, characterized by negligible photocurrent at voltages up to ~0.5 V negative of the flatband potential (~0.1 V vs. SCE). A marked hysteresis in S values is observed in the PA potential regime of -0.1 to -0.4 V vs. SCE. Estimated S values are high, approaching 10^7 cm/s, but decrease significantly during anodic-going scans. Variations in W between -0.1 and -0.8 V vs. SCE indicate that strong Fermi-level pinning does not obtain. Electrode operation under a pulsed potential program (-0.05 to -1.00 V vs. SCE) caused a transient reduction in S of approximately an order of magnitude.

(Keywords: ... appear ... 10 to the 7th power ...)

20. DISTRIBUTION / AVAILABILITY OF ABSTRACT	21. ABSTRACT SECURITY CLASSIFICATION
☒ UNCLASSIFIED/UNLIMITED ☐ SAME AS RPT. ☐ DTIC USERS	Distribution Unlimited
22a. NAME OF RESPONSIBLE INDIVIDUAL Arthur B. Ellis	22b. TELEPHONE (Include Area Code) 608-262-0421 / 22c. OFFICE SYMBOL

DD FORM 1473, 84 MAR — 83 APR edition may be used until exhausted. All other editions are obsolete.

SECURITY CLASSIFICATION OF THIS PAGE
Unclassified

I. INTRODUCTION

Photoluminescence (PL) techniques offer unique advantages for the study of photoelectrochemical cells (PEC's). The PL intensity of semiconductors is sensitive to the depletion width W in the semiconductor and to the rate of minority carrier loss at the surface S. A simple dead-layer model (DLM)[1] has been employed to relate changes in the steady-state PL intensity of a variety of semiconductor electrodes to changes in W.[2-6] Both pulsed[7] and steady-state[8,9] PL intensity measurements have been interpreted in terms of changes in S. Recently, we have shown that a PL model developed by Mettler[10] is capable of simultaneously assessing values of W and S as a function of electrode potential. The model was applied to n-GaAs electrodes in PEC's employing aqueous telluride electrolyte.[11]

The non-idealities in the photoelectrochemical behavior of p-type III-V semiconductors have been the subject of several studies.[12-16] Of particular interest is the "photocurrent anomaly" (PA), a 0.4 to 0.6 V separation of the photocurrent onset from the flatband potential.[14] As a consequence of this overpotential, the onset of cathodic currents leading to hydrogen evolution is close to that of conventional metal electrodes[13] and much of the theoretical efficiency for converting optical to chemical energy is lost.

For PEC's employing p-GaAs or p-GaP electrodes in H_2SO_4 electrolyte, several theories have been advanced to account for the observed PA. In one study, a thermally-limited value of S was a suggested contributor to the effect.[14] Another study attributed the PA to increases in S at potentials near the flat-band potential V_{fb}.

due to the corresponding higher concentration of majority carriers at the surface.[13] Also relevant to an understanding of the PA is Fermi-level pinning, which has been proposed for aqueous p-GaAs PEC's.[12,17] Transient PL effects have been ascribed to a shift in band edges in the PA potential regime.[6]

We report herein on the steady-state and transient PL properties of a p-GaAs-based PEC employing an aqueous acidic electrolyte. Our results reveal that over the potential regime corresponding to the PA, values of S show considerable hysteresis; the values are high, maximally approximating the thermal limit. Furthermore, significant variations in W observed between -0.1 and -0.8 V vs. SCE indicate that the electrode is not strongly pinned. Operating the electrode under a pulsed potential program causes a transient reduction in S of approximately an order of magnitude.

II. THEORY

A simple dead-layer model (DLM) has been used to estimate changes in W from PL quenching data: The model assumes that electron-hole pairs formed within a distance on the order of W do not radiatively recombine.[1] Thus, a change in dead-layer thickness ΔD as a function of applied potential is expressed by Eq. (1),

$$\Delta D = (-1/\alpha') \ln(PL_1/PL_2), \qquad [1]$$

where $\alpha' = (\alpha_e + \alpha_p)$ is the sum of the absorptivities of the semiconductor for the excitation and emission wavelengths, respectively; and PL_1 and PL_2 are PL intensities at two arbitrary potentials for which the semiconductor is in depletion. If one of the

electrode potentials is V_{fb}, then the total dead-layer thickness, approximating the depletion width, may be obtained. The DLM is valid under conditions of high or constant virtual surface recombination velocity S.[2]

Use of ΔD values as a lower limit for W in Eq. (2) yields an approximate lower limit for the Schottky barrier height V_B of the semiconductor-electrolyte interface. In this expression, ϵ is the dielectric constant of the semiconductor (12.9 for GaAs[18]), ϵ_o is the permittivity

$$W = (2\epsilon\epsilon_o V_B/qN_A)^{1/2} \qquad [2]$$

of vacuum; q is the electronic charge; and N_A is the acceptor concentration.

Despite its strengths, the DLM's inability to accommodate significant changes in S or to yield absolute depletion widths restricts its applicability. A more powerful methodology was developed by Mettler for the analysis of PL fromGaAs in air.[10] His treatment, encompassing both the dead-layer formalism and the influence of minority carrier loss at the surface upon PL intensity, results in Eq. (3). In this equation, I_L is the observed

$$I_L = K \exp[-(\alpha_e+\alpha_p)W] \frac{\alpha_e L_n}{(\alpha_e L_n)^2 - 1} \cdot \qquad [3]$$

$$\times \left(\frac{S_r+\alpha_e L_n}{(S_r+1)(\alpha_p L_n+1)} - \frac{1}{(\alpha_e+\alpha_p)L_n} \right)$$

PL intensity divided by the excitation intensity, corrected for

reflective losses; K is a constant containing the internal quantum efficiency and geometrical factors involved in light collection; L_n is the electron diffusion length; and S_r is the reduced surface electron-capture velocity. The reduced velocity is a dimensionless parameter related to the more commonly determined surface electron-capture velocity S by Eq. (4), where τ_n is the electron lifetime. Our use of the term

$$S_r = S(\tau_n/L_n) \qquad [4]$$

"surface electron-capture velocity" rather than the conventional term "surface recombination velocity" used by Mettler reflects the fact that additional pathways for surface recombination involving interfacial charge transfer are available in a PEC.

The derivation of Eq. (3) assumes that the optical penetration depth (OPD) is significantly less than the minority carrier diffusion length, i.e., $\alpha_e^{-1} < L_n$. Given an estimate of L_n, a plot of I_L vs. α_e^{-1} (I_L-OPD plots) can be fit to Eq. (3) to obtain both W and S_r. The value of W obtained can be used to approximate the Schottky barrier height V_B with Eq. (2) (vide supra).

Data acquired at different potentials is analyzed by using the solution of Eq. (3) (shape fit) obtained at one potential V_1 as a reference. A ratio Q, formed with the V_1 data and data obtained at another potential V_2, is fit to Eq. (5) (ratio fits). As expected, Eq. (5)

$$Q = \frac{I_L(V_1)}{I_L(V_2)} = \exp\left[-(\alpha_e+\alpha_p)(W(V_1)-W(V_2))\right] \cdot \frac{[\ ]V_1}{[\ ]V_2} \qquad [5]$$

where $$[\ ]_V = \frac{S_r(V) + \alpha_e L_n}{(S_r(V)+1)(\alpha_p L_n+1)} - \frac{1}{(\alpha_e+\alpha_p)L_n}$$

reduces to Eq. (1) if S_r is relatively large ($S_r \gg 1$ and $\alpha_e L_n$) or independent of the applied potential.[2] Our use of ratios (Q-OPD plots) rather than individual I_L-OPD plots leads to smaller standard deviations in W and S_r.

Use of these equations requires absorptivities α_e, reflectivities, and an estimate of L_n. The absorptivities used for p-GaAs were those employed in the study of n-GaAs electrodes.[11] An absorptivity of 9×10^3 cm^{-1} was used for the emitted light, monitored at 865 nm.[19] For data acquired in solution, literature reflectivities[20] were corrected for the refractive index of the electrolyte.

Literature values for L_n in melt-grown or diffused p-GaAs:Zn vary[21-23], but reasonable estimates for use in Eqs. (3) and (5) are 5 μm for $p = 3.1 \times 10^{17}$ cm^{-3}, 4 μm for $p = 1 \times 10^{18}$ cm^{-3}, and 3 μm for $p = 1.8 \times 10^{19}$ cm^{-3}. The qualitative aspects of this analysis are unaffected by this parameter, although the data cannot be fit if very small (< 1 μm) values of L_n are used. Larger values of L_n yield larger calculated W and S_r values. Values of W are relatively insensitive to the value of L_n chosen; however, calculated values of S_r are nearly proportional to the L_n value employed.

III. EXPERIMENT

The p-GaAs samples used in this study were melt-grown samples obtained from Laser Diode Laboratories (Cd doped, (111), 3.1×10^{17} cm^{-3}), Atomergic Chemicals, Inc. (Zn doped, (111), 1.0×10^{18} cm^{-3}), and Morgan Semiconductor, Inc. (Zn doped, $1/2^0$ off (100), 1.8×10^{19} cm^{-3}). The (111)-oriented samples were received with a polished "B"-face (As face), and this surface was used in our experiments. The orientation of the (111) samples was determined

by chemical etching and optical microscopy.[24] Ohmic contacts to the crystals (~ 0.5 x 0.5 x 0.1 mm^3) were made by soldering a HgInZn eutectic to the back of the crystal. Crystals were then mounted as described elsewhere.[25] Before use in a PEC, electrodes were etched in a room temperature 3:1:1 H_2SO_4:H_2O_2(30%):H_2O solution, followed by rinsing with NH_4OH and triply-distilled (3D) water.

The electrolyte was prepared from H_2SO_4 (Mallinckrodt analytical reagent grade or Alfa Products Ultrapure gave similar results) and KSCN (Baker, reagent grade). All solutions were deoxygenated with N_2 for at least 30 min. before use, bubbled and blanketed with N_2 during use, and magnetically stirred.

Luminescence-voltage (L-V) and current-voltage (i-V) curves were obtained by cycling between -0.05 V and -0.85 V vs. SCE at 10 mV/s using a standard three-electrode potentiostatic setup and electrochemical equipment described previously.[25] Front-surface PL was monitored at the uncorrected band maximum of 865 nm. The experimental apparatus is as described previously, [11] except for the use of a lamp/monochromator assembly. Illumination was accomplished with a Photon Technologies Inc. Model 01-150 high-intensity illumination system, which includes a Model 01-150X1 150 W Xe lamp, an elliptical mirror, and a Model 01-001 0.25-m monochromator. This excitation system permits computer control of the wavelength scan rate and entrance slit, the latter providing control of the system's output intensity. The output was kept roughly photon-matched and the uncorrected measured bandpass of the system was typically ~10 nm over the 450-690 nm spectral range used. The intensity at the sample surface with 570 nm excitation was ~1.5 mW/cm^2. A Melles-Griot hot mirror (03 MHG 007) was placed at the exit slit of the excitation monochromator to

reduce near-infrared interference (> ~700 nm) with the PL signal. A polarizing filter was also used to prevent spectral variations in the excitation polarization.

The program for the pulsed-potential experiments (toggling between -0.05 V (0.5 s) and -1.0 V vs. SCE (0.5 s)) was provided by an EG&G PARC Model 175 Universal Programmer and Model 173/176 Potentiostat/Current Follower. PL intensity for the pulse experiments was obtained with an EG&G ORTEC Model 9349 Log/Lin Ratemeter, used to monitor the amplifier/discriminator, and a Linseis LY 18100 X(T)-Y recorder operated in time base mode. The system response time was estimated at <0.2 s.

A difficulty in characterizing the p-GaAs PL is posed by its temporal instability during photoelectrochemical operation. As described in the text, addition of KSCN to the electrolyte improves the long-term stability of L-V behavior. Reproducible I_L-OPD curves were typically obtained by cycling the electrode between -0.05 V and -0.85 V with excitation at 450 nm for at least 45 min. prior to the acquisition of data for the plots; by acquiring the data over 30 nm intervals rather than the 10 nm intervals used in air or at open circuit; and by performing ratio fits (Q-OPD plots, Eq. (5)) relative to data obtained at -0.8 V on the cathodic-going scan, a potential for which I_L-OPD curves exhibited the least change with time. The generated I_L-OPD and Q-OPD curves were fit using a nonlinear least-squares curve-fitting program.

III. RESULTS

A. PL properties in a PEC

Typical luminescence-voltage (L-V) and current-voltage (i-V) curves for a p-GaAs electrode ($p = 5.1 \times 10^{17}$ cm^{-3}) in aqueous H_2SO_4

electrolyte are shown in Fig. 1. The PL intensity, shown over one-and-a-half cycles, exhibits a substantial enhancement between the first and second cycles as well as considerable hysteresis between anodic- and cathodic-going scans. The potential regime most affected is from ~-0.4 to 0.0 V vs. SCE. As shown in the bottom panel of Fig. 1, this is just the regime corresponding to the "photocurrent anomaly" (PA): negligible Faradaic current flows between the estimated flatband potential, under illumination, of 0.1 V vs. SCE[14] and -0.4 V. We will show that the PL effects derive largely from changes in the reduced surface electron-capture velocity S_r over the PA potential regime, although some contribution from a change in W cannot be excluded.

With continued cycling between -0.05 V and -0.85 V, the PL settles into the patterns shown in Fig. 2. These plots were obtained in the presence of KSCN, which markedly improved the long-term stability of the data; the salt is reported to aid the reversibility of Ga plating[26] and to assist the anodic dissolution of Ga from GaAs surfaces.[27] The figure emphasizes the greater relative hysteresis at shorter excitation wavelengths, implying that surface chemistry causes the hysteresis (vide infra).

Electrode reflectance was monitored over several cycles to discern whether the PL changes were attributable to this parameter. No changes were observed within the error (± 2% relative) of the experiment. The variations in PL thus result from changes in W, S_r, or both.

An analysis using Mettler's methodology provides a means for obtaining S_r and W as a function of applied potential. Typical I_L-OPD plots for a p-GaAs electrode at -0.1 V (anodic-going) and -0.8 V (cathodic-going) vs. SCE are shown in Fig. 3. Good fits are

obtained to Eq. (3) for both . A ratio fit (Q-OPD plot) using Eq. (5) for the data at -0.1 V was somewhat less satisfactory , although it resulted in similar values for W and S_r.

The discrepancy observed with the ratio fit is likely due to errors of several percent in the relative spectral response of the apparatus and/or in the absorptivities and reflectivities of the semiconductor. Occasionally, small negative values for W are obtained, but they are within experimental error of zero.

Values of W and S_r, extracted from the curves of Fig. 3 and from Q-OPD curves at other potentials, are compiled in Table I and plotted in Fig. 4. A comparison of the values for W and S_r for the two scan directions indicates that the PL intensity in the PA regime is affected by changes in both parameters: On the cathodic-going scan, W increases modestly by ~100 Å, but S_r increases by a factor of two between ~-0.1 and -0.4 V; similar values are obtained in the PA regime on the anodic-going scan, although corresponding values for S_r are consistently lower. The discrepancy in S_r for the two scan directions can account for the hysteresis observed, although we cannot exclude some contribution from W, due to the uncertainty in our measurements. It is noteworthy that the hysteresis in PL intensity and in S_r occurs in the region of negligible photocurrent where conventional surface recombination and not Faradaic charge transfer is the dominant form of minority carrier relaxation at the interface. The change in S_r implicates changes in the chemical nature of the surface. The magnitude of S_r is also of interest. Our maximum values of nearly 100 correspond to values for S, using Eq. (4) and literature electron lifetimes (~10^{-9} s)[21,23] and diffusion lengths (1-5 μm), that approximate the thermal limit of ~10^7 cm/s.

In principle, values of W permit an assessment of the manner

in which applied potential is partitioned across the semiconductor-electrolyte interface. Although such an analysis must be tempered by the uncertainty in W, values of W are smaller than would be expected based on the flatband potential of ~0.1 V vs. SCE reported for illuminated p-GaAs.[14] Assuming ideal behavior, Eq. (2) predicts that W will change most rapidly with potential at potentials near V_{fb}. Data in Table I exhibit the opposite trend, indicating that partitioning of applied potential occurs at the more positive potentials sampled. Beyond the PA potential regime, as the electrode potential passes from -0.4 to -0.8 V, W increases from 80 to 360 A; this corresponds to a 0.3 V increase in Schottky barrier height for a 0.4-V increment of applied potential.

Data obtained on more conductive samples ($p = 1.0 \times 10^{18}$ and 1.8×10^{19} cm^{-3}) exhibit the same trends in W and S_T but generally indicate larger barriers and barrier height changes with applied potential. As a result of the linear relationship between carrier concentration and barrier height (Eq. (2)), errors in W increase with p. Thus, although the calculated barriers may exceed those theoretically possible for GaAs (i.e., $V_B > E_g$), perfectly reasonable barriers exist within the uncertainties of the measurement. In this context it is worth examining results found with the simple dead-layer model (DLM). Table I shows that values for ΔD from Eq. (1) are considerably larger than the corresponding values for W obtained using Mettler's treatment. In many cases the ΔD values correspond to physically unreasonable changes in barrier height, a consequence of interpreting the PL changes exclusively in terms of changes in the width of the space-charge region.

B. Transient PL effects

As shown in Fig. 1, an initial cycling of the p-GaAs electrode produces a substantial enhancement in PL intensity in the PA potential regime. A related observation was made by Uosaki, et al: transient PL enhancements were observed upon pulsing p-GaAs electrodes from -1.0 V to rest potentials positive of or equal to -0.35 V vs. Ag/AgCl in 0.5 M H_2SO_4 electrolyte.[6] We have examined the transient PL enhancements and demonstrate below that they are accompanied by a significant reduction in S_r.

Brief operation of a freshly etched electrode cathodic of ~-0.4 V vs. SCE yields a transient increase in PL intensity when the electrode is subsequently taken out of circuit or brought to a potential near the open-circuit voltage (OCV) of 0.1 to 0.2 V. Much of the PL enhancement decays within seconds of the positive-going pulse, although some enhancement persists for minutes. The magnitude of the PL increase varies with the extent of etching and with the duration and potential of the cathodic excursion; the PL transient increased in intensity with more cathodic potentials up to -1.0 V.

Repetitive pulsing between a cathodic potential (-1.00 V for 0.5 s) and a potential slightly negative of the OCV (-0.05 V for 0.5 s) produces a maximum enhancement in PL intensity after several minutes, as shown in Fig. 5. This maximum intensity was sufficiently stable to permit acquisition of I_L-OPD plots. Ratio fits were then obtained relative to data obtained at the OCV prior to commencing the pulse program. Representative data are shown in Fig. 6.

Analysis of the Fig. 6 data reveals that S_r declines by an order of magnitude, from ~90 at OCV before the pulse program to ~6 at

-0.05 V after the pulse program; values for W were within experimental error of zero in both measurements. During the experiment, the PL intensity at -1.00 V remains constant to within 10% while the PL intensity at -0.05 V increases roughly six-fold. This indicates that W and S_r at -1.00 V (~280 Å and 90, respectively, for the experiment of Fig. 6) are negligibly affected by the experiment.

IV. DISCUSSION

Our PL data indicate that significant changes in S_r occur in the photocurrent anomaly (PA) regime of p-GaAs-based PEC's employing aqueous H_2SO_4 electrolyte. These changes are evident in both long-term cyclic voltammetric scans and in pulsed potential experiments. The PL data prompt consideration of the surface chemistry that could alter the number and/or location of surface states mediating recombination. Two possibilities are chemistry associated with hydrogen evolution and semiconductor redox processes. The approximate "onset" potential of the PL transient behavior and of the hysteresis in L-V plots (-0.4 V vs. SCE) corresponds to the onset of cathodic current for hydrogen evolution[28], suggesting that surface coverage by hydrogen atoms may influence PL.

Alternatively, changes in S_r could involve the preferential reductive removal of surface As. Woodall, et. al. have recently used photochemical methods to temporarily remove surface states from n- and p-GaAs.[29] The change was attributed to the photochemical removal of As and/or As_2O_3 and their associated surface states, with possible inhibition of the surface degradation by a gallium oxide layer; the possibility of an oxide-free surface was

not ruled out. Our results may reflect analogous variations in the density of As-related surface states. In this scenario, the cathodic portion of the cycle could be interpreted as allowing preferential removal of surface As, and the anodic portion as creating a transient protective gallium oxide.

Turning to the values of W obtained, we note that they are in accord with existing capacitance studies,[14,30] which indicate that strong Fermi-level pinning (fixed V_B and hence W) is not a prevalent mechanism for p-GaAs in acidic aqueous electrolyte. A 200-mV positive band edge shift under illumination was inferred by Kelly and Memming from capacitance measurements as the electrode potential nears V_{fb}. Uosaki et. al. explained their PL transients, observed following a positive-going potential pulse, in terms of such a shift. The band edge shift was attributed to surface chemistry in that study.[6] Our results are not inconsistent with some partitioning of applied potential. They also indicate that changes in S, derived from surface chemistry, play a crucial role in transient PL behavior.

A thermally limited value of S_r in the PA regime had been estimated previously by Kelly and Memming.[14] Although we find that S_r varies significantly in the PA regime, our maximum values do approach the thermal limit of ~10^7 cm/s. Particularly intriguing is the order-of-magnitude reduction in S_r found by pulsing the electrode across the PA potential regime. If the reduction in S_r is due to the removal or shifting of surface states, then it is possible that surface treatment during a pulsing program could preserve the effect. Whether this could facilitate interfacial charge transfer is hard to predict. Improvements to date in p-type III-V photocurrent properties have come from using redox couples with

better kinetics than the hydrogen evolution reaction[14] or by enhancing the hydrogen evolution kinetics by metal[13] or metal ion treatment.[15,16]

V. CONCLUSIONS

The PL from p-GaAs photocathodes employed in aqueous sulfuric acid electrolyte has been used to monitor the depletion width W and surface electron-capture velocity S while the electrode serves as the photocathode in an operating PEC. In the region of the photocurrent anomaly (between ~-0.1 and -0.4 V vs. SCE), hysteresis in the PL intensity correlates with hysteresis in values of S. Values of S are near the thermal limit. Repetitive pulsing of the electrode potential between -0.05 and -1.00V vs. SCE yields an order-of-magnitude reduction in S. Variations in W between -0.1 and -0.8 V vs. SCE indicate that the electrode is not strongly Fermi-level pinned, but uncertainties in W preclude a more detailed analysis of the partitioning of applied potential across the p-GaAs-electrolyte interface.

ACKNOWLEDGMENTS

The authors thank the Office of Naval Research and the University of Wisconsin-Madison, University-Industry Research Program for support of this research. We thank Laura Becker of Laser Diodes, Inc. and Alan Huelsman of MIT for Hall measurements.

REFERENCES

1. R. E. Hollingsworth and J. R. Sites, J. Appl. Phys., 53, 5357 (1982) and references therein.

2. W. S. Hobson and A. B. Ellis, J. Appl. Phys., 54, 5956 (1983).

3. R. Garuthara, M.Tomkiewicz, and R.P.Silberstein, J. Appl. Phys., 54 , 6787 (1983)

4. W. S. Hobson, P. B. Johnson, A. B. Ellis, and R. M. Biefeld, Appl. Phys. Lett., 45, 150 (1984).

5. P. B. Johnson, A. B. Ellis, R. M. Biefeld, and D. S. Ginley, Appl. Phys. Lett., 47, 877 (1985).

6. S. Kaneko, K. Uosaki, and H. Kita, Chem, Lett., 1951, (1986).

7. M. Evenor, S. Gottesfeld, Z. Harion, D. Hupper, and S.W. Feldberg, J. Phys. Chem., 88 , 6215 (1984)

8. K.H. Beckmann and R. Memming, J. Electrochem. Soc., 116 , 368 (1969)

9. A. Etcheberry, J. Gautron, and J. L. Sculfort, Appl. Phys. Lett., 46, 744 (1985).

10. K. Mettler, Appl. Phys., 12, 75 (1977)

11. A. A. Burk, Jr., P. B. Johnson, W. S. Hobson, and A. B. Ellis, J. Appl. Phys., 59, 1621 (1986).

12. F.-R. F. Fan and A. J. Bard, J. Am. Chem. Soc., 102, 3677 (1980).

13. Y. Nakato, S. Tonomura, and H. Tsubomura, Ber. Bunsenges. Phys. Chem., 80, 1289 (1976)

14. J. J. Kelly and R. Memming, J. Electrochem. Soc., 129, 730 (1982).

15. K. Uosaki and H. Kita, Chem. Lett. 953 (1984).

16. M. P. Dare-Edwards, A. Hamnett, and J. B. Goodenough, J. Electroanal. Chem., 119, 109 (1981).

17. J. O'M. Bockris and S. U. M. Khan, Appl. Phys. Lett., 42, 124 (1983)

18. G. E. Stillman, C. M. Wolfe, and J. O. Dimmock in "Semiconductors and Semimetals," R. K. Willardson and A. C. Beer, Eds., Academic: New York, 1977, Vol. 12, p. 169.

19. M. D. Sturge, Phys. Rev., 127, 768 (1962).

20. B. O. Seraphin and H. E. Bennett, in "Semiconductors and Semimetals," R. K. Willardson and A. C. Beer, Eds., Academic: New York, 1967, Vol. 3, p.499.

21. J. Vilms and W. E. Spicer, J. Appl. Phys., 36, 2815 (1965).

22. L. Jastrzebski, H.C. Gatos, and J. Lagowski, J. Appl. Phys., 48, 1750 (1977).

23. L.W. Aukerman, M.F. Millea, and M. McColl, J. Appl. Phys. 38, 685 (1967).

24. D. F. Kyser and M. F. Millea, J. Electrochem. Soc., 111, 1102 (1964).

25. B. R. Karas and A. B. Ellis, J. Am. Chem. Soc., 102, 968 (1980).

26. E. D. Moorhead, J. Am. Chem. Soc., 87, 2503 (1965).

27. F. W. Ostermayer, Jr. and P. A. Kohl, Appl. Phys. Lett., 39, 76 (1981).

28. H. Gerischer, N. Muller, and O. Haas, J. Electroanal. Chem., 119, 41 (1981), and references therein.

29. S. D. Offsey, J. M. Woodall, A. C. Warren, P. D. Kirchner, T. I. Chappell, and G. D. Pettit, Appl. Phys. Lett., 48, 475 (1986)

30. W. H. Laflere, R. L. Van Meirhaeghe, and F. Cardon, Surface Science, 59, 401 (1976).

Table I. Electrode Parameters of a p-GaAs-based PEC[a]

Volts vs. SCE[b]	W (Å)[c]	ΔD (Å)[d]	S_r[e]	Volts vs. SCE[b]	W (Å)[c]	ΔD (Å)[d]	S_r[e]
(-) - 0.1	- 10	200	42	(+) - 0.1	0	0	32
(-) - 0.2	20	330	51	(+) - 0.2	-20	70	37
(-) - 0.3	30	400	59	(+) - 0.3	30	260	46
(-) - 0.4	80	510	66	(+) - 0.4	110	450	61
(-) - 0.5	180	610	70	(+) - 0.5	210	630	73
(-) - 0.6	220	710	78	(+) - 0.6	260	710	77
(-) - 0.7	310	750	73	(+) - 0.7	310	760	79
(-) - 0.8	359	810	72	(+) - 0.8	340	820	84
OCV[f]	50	—	78				

[a] Properties derived from the PL of a p-GaAs electrode, (111) As-rich face, with $p = 3.1 \times 10^{17}$ cm^{-3}. The PEC consisted of a three-electrode potentiostatic setup and a 0.5 M H_2SO_4/0.1 M KSCN electrolyte. Table entries are extracted from Q-OPD plots like that shown in Fig. 3. Magnetic stirring, a N_2 blanket, and slow N_2 bubbling were used in all PEC experiments. Bold-faced numbers are data acquired at the potential to which ratio fits (Eq. (5)) are referenced. Agreement between shape fits (Eq. (3)) and the ratio results tabulated here (Eq. (5)) was generally good. The influence of uncertainties in L_n on the table entries is discussed in the text.

[b] Potential of the p-GaAs electrode; the symbol preceding the voltage indicates a cathodic-going (-) or anodic-going (+) scan.

[c] Depletion width at the indicated potential, obtained by fitting Q-OPD curves to Eq. (5); at the reference potential of (-) -0.8 V

vs. SCE, W is obtained by fitting the I_L-OPD curve to Eq. (3). The standard deviation of the nonlinear least-squares fit for the reference value was ± 110 A. The relative error between two values on the table is typically ±20-60 A., with the larger uncertainties in the region of hysteresis. Negative values reflect the uncertainty in the determination of W.

[d] Change in dead-layer thickness relative to the value for (+) -0.1 V vs. SCE. The values listed are those calculated for 570-nm excitation.

[e] Reduced surface electron-capture velocity at the indicated potential, obtained by fitting Q-OPD curves to Eq. (5); at the reference potential of (-) -0.8 V vs. SCE, S_r was calculated using Eq. (3). The standard deviation of the nonlinear least-squares fit for the reference value was ± 31. The relative error between two values in the table is typically ±5-9.

[f] The value obtained at open circuit (0.17 V vs. SCE) prior to cycling the electrode's voltage.

Figure 1. Relative photocurrent (bottom panel) and PL intensity (top panel) as a function of electrode potential for a p-GaAs-based PEC employing 0.5 M H_2SO_4 electrolyte; PL intensity was monitored at λ_{max}, 865 nm. The electrode (p = 3.1 x 10^{17} cm^{-3}) was excited with ~1.5 mW/cm^2 of 450-nm light. The first and second cathodic-going scans of PL intensity are labeled A and B, respectively; the photocurrent is only shown for the initial scan. The curves were swept simultaneously at 10 mV/s.

Figure 2. Photoluminescence intensity as a function of electrode potential for three excitation wavelengths, 450, 570, and 690 nm. Data were obtained for a p-GaAs electrode (p=3.1x10^{17} cm^{-3}) in 0.5 M H_2SO_4/0.1 M KSCN electrolyte after cycling continuously for 4 h between -0.05 and -0.85 V vs. SCE at 10 mV/s. The three panels do not have the same vertical scale.

Figure 3. Photoluminescence intensity vs. optical penetration depth (I_L-OPD) curves for a p-GaAs electrode (p = 3.1 x 10^{17} cm^{-3}) in 0.5 M H_2SO_4/0.1 M KSCN electrolyte at two electrode potentials, -0.1 V (squares; acquired for an anodic-going scan) and -0.8 V vs. SCE (circles; acquired for a cathodic-going scan). Values of S_r and W extracted at these potentials are given in Table I. The solid line passing through data at -0.8 V and the dashed line at -0.1 V are best fits to Eq. (3). The solid line passing through data at -0.1 V is the best fit to Eq. (5)

Figure 4. Calculated values of S_r and W as a function of electrode potential. Values from the cathodic-going scans are denoted by squares and those from anodic-going scans by circles. Parameters calculated for -0.8 V on the cathodic-going scan serve as the reference values. The error bars for the reference values reflect the uncertainty in the absolute values and the other error bars reflect the uncertainty in the relative values.

Figure 5. Growth in PL intensity caused by electrode pulsing. The p-GaAs electrode ($p = 3.1 \times 10^{17}$ cm^{-3}) was operated in 0.5 M H_2SO_4/0.1 M KSCN electrolyte with 450-nm excitation. PL intensity for times preceding t = 0 is that of a freshly etched electrode at open circuit; after t = 0, the data are the end points of the recorder pen's deflection, obtained while pulsing the electrode potential between -0.05 V vs. SCE (0.5 s), the top curve, and -1.00 V vs. SCE (0.5 s), the lower curve.

Figure 6. Photoluminescence (PL) intensity vs. optical penetration depth (I_L-OPD curves) for a p-GaAs electrode ($p = 3.1 \times 10^{17}$ cm^{-3}) in 0.5 M H_2SO_4 electrolyte before being placed in circuit (circles) and at -0.05 V vs. SCE after being repetitively pulsed, as described in Fig. (5), until the PL enhancement had saturated (squares). Values of S_r and W extracted at these potentials are presented in the text. The solid lines are the best fit to Eq. (3) for the open-circuit data and the best fit to Eq. (5) for the -0.05 V data.

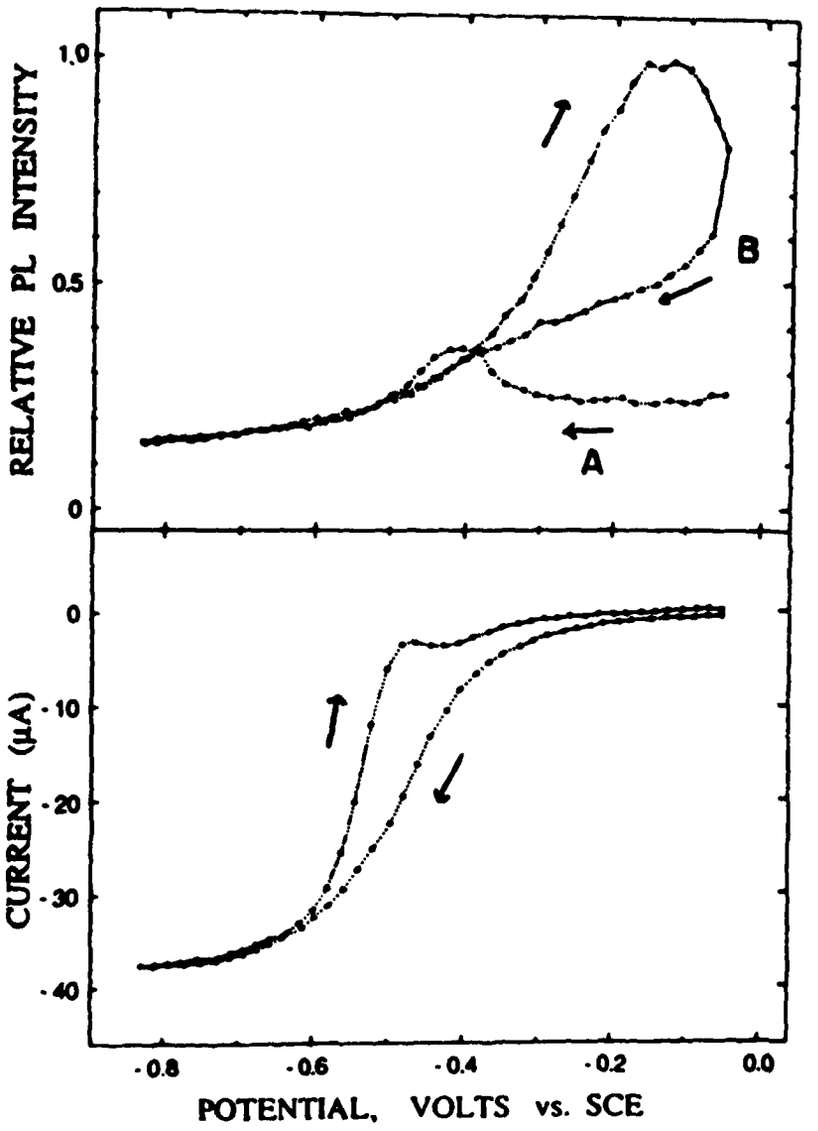
RELATIVE PL INTENSITY
1.0
0.5
0
B
A
CURRENT (μA)
0
-10
-20
-30
-40
-0.8
-0.6
-0.4
-0.2
0.0
POTENTIAL, VOLTS vs. SCE

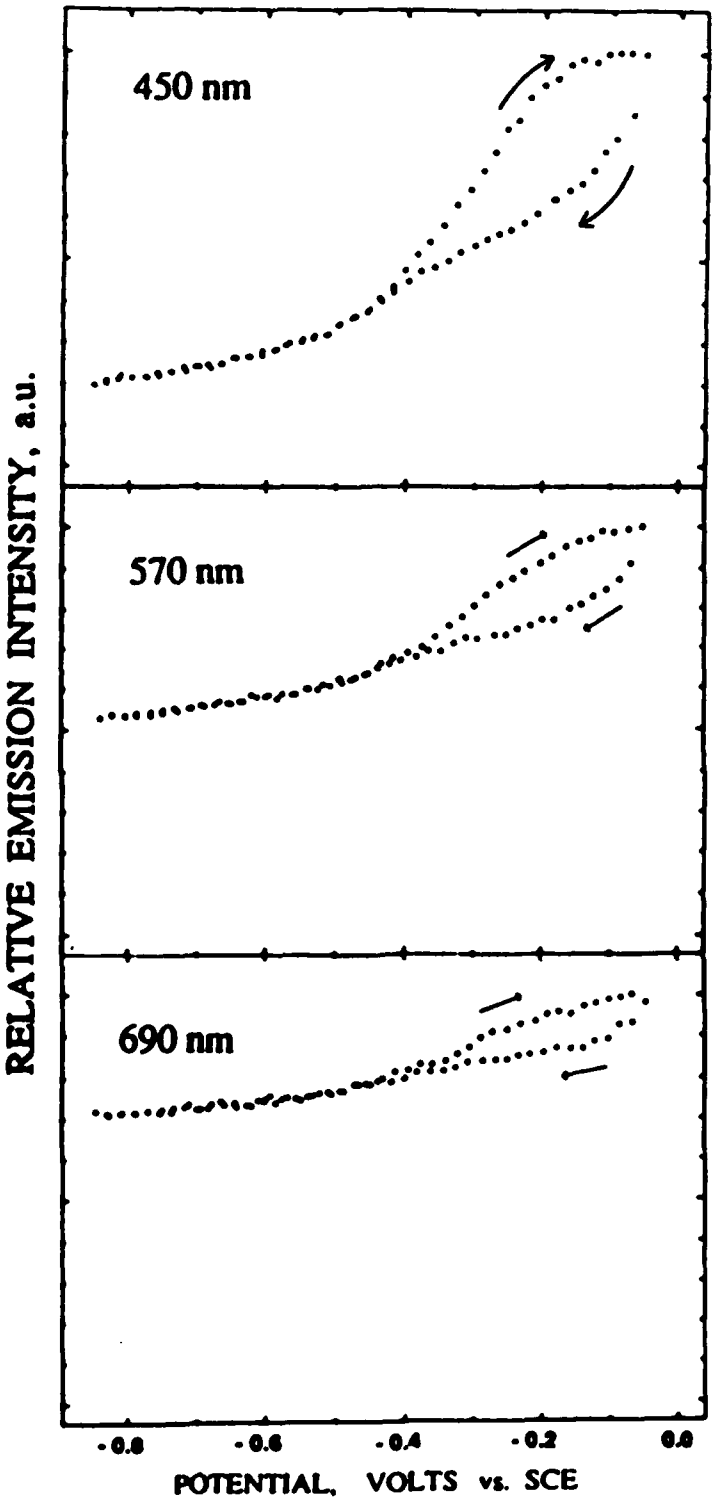
450 nm
570 nm
690 nm
RELATIVE EMISSION INTENSITY, a.u.
-0.8
-0.6
-0.4
-0.2
0.0
POTENTIAL, VOLTS vs. SCE

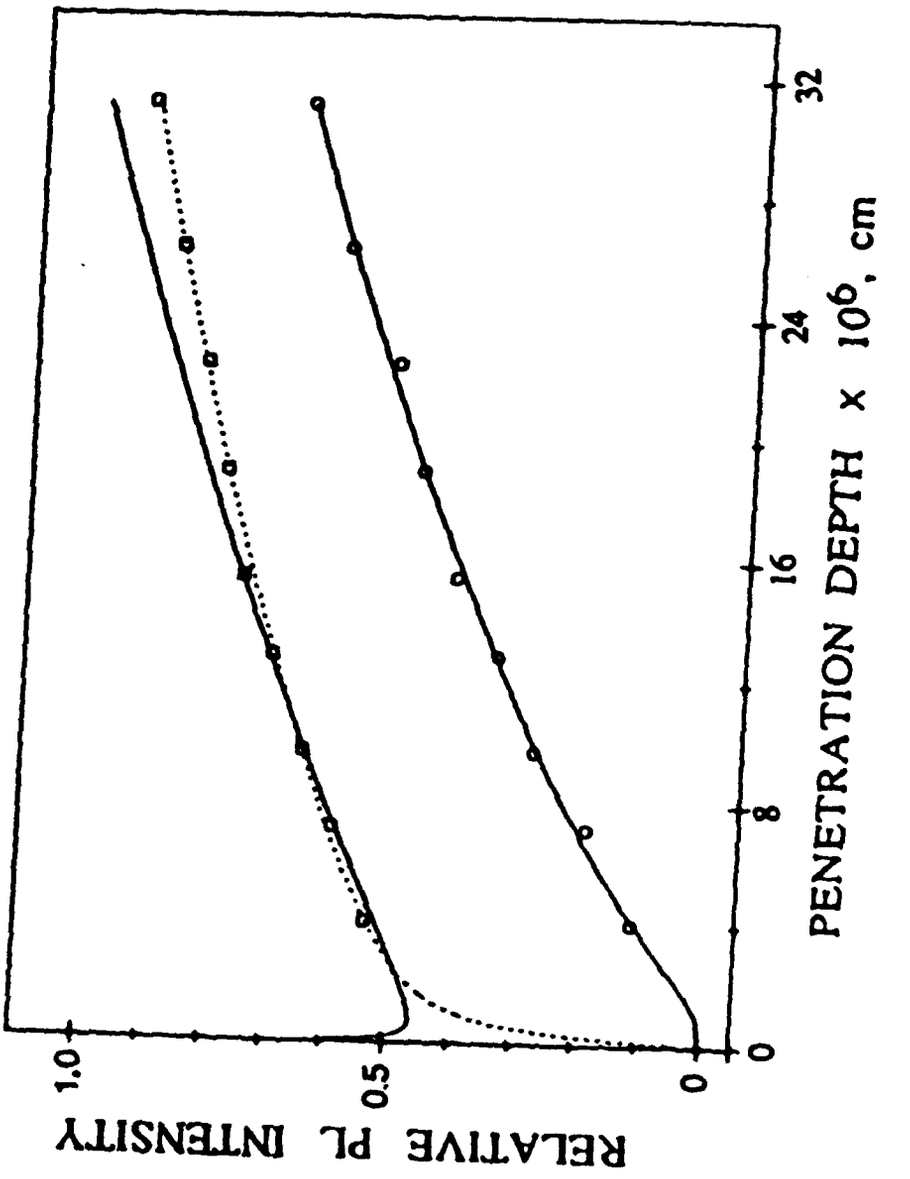
RELATIVE PL INTENSITY
1.0
0.5
0
0
8
16
24
32
PENETRATION DEPTH x 10^6, cm

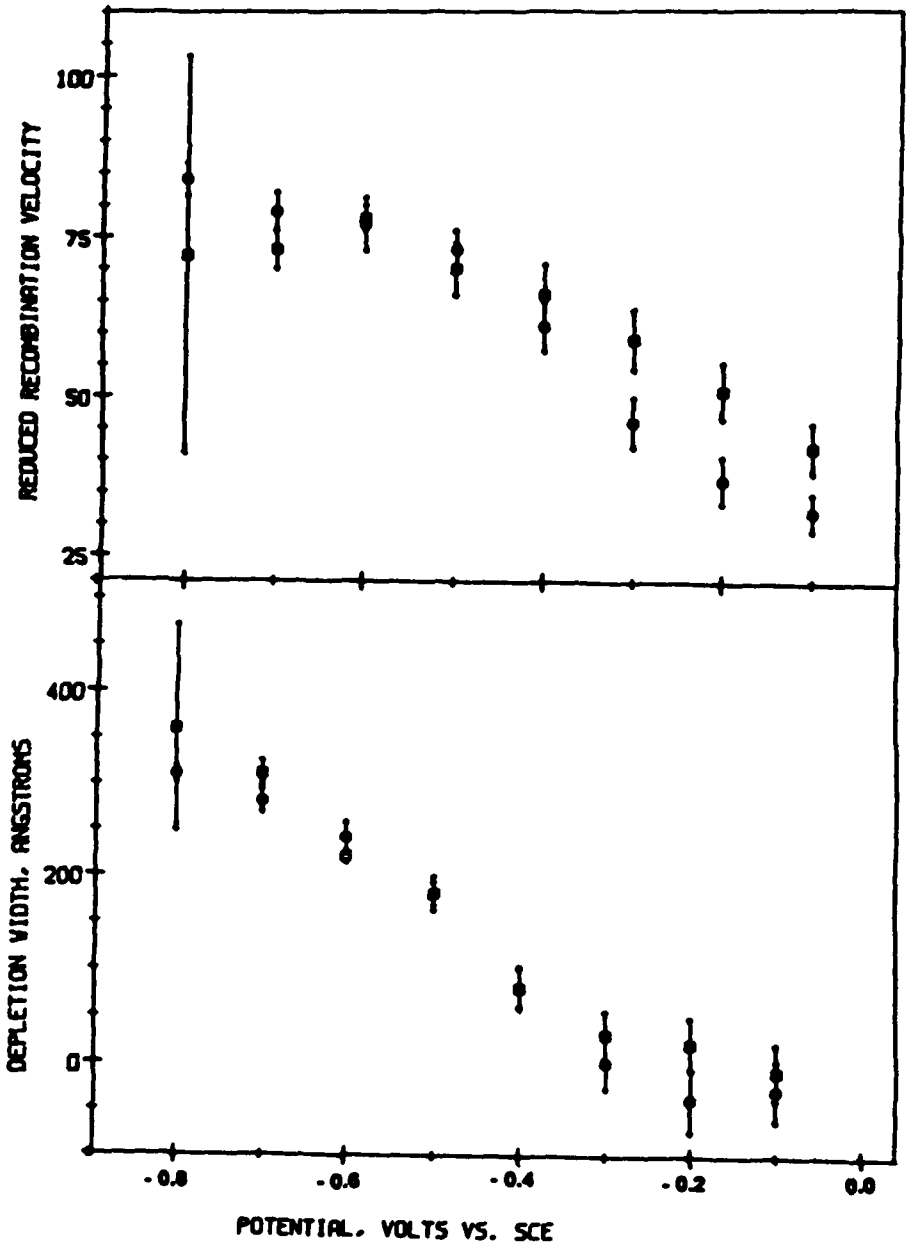
REDUCED RECOMBINATION VELOCITY
100
75
50
25
DEPLETION WIDTH, ANGSTROMS
400
200
0
-0.8
-0.6
-0.4
-0.2
0.0
POTENTIAL, VOLTS VS. SCE

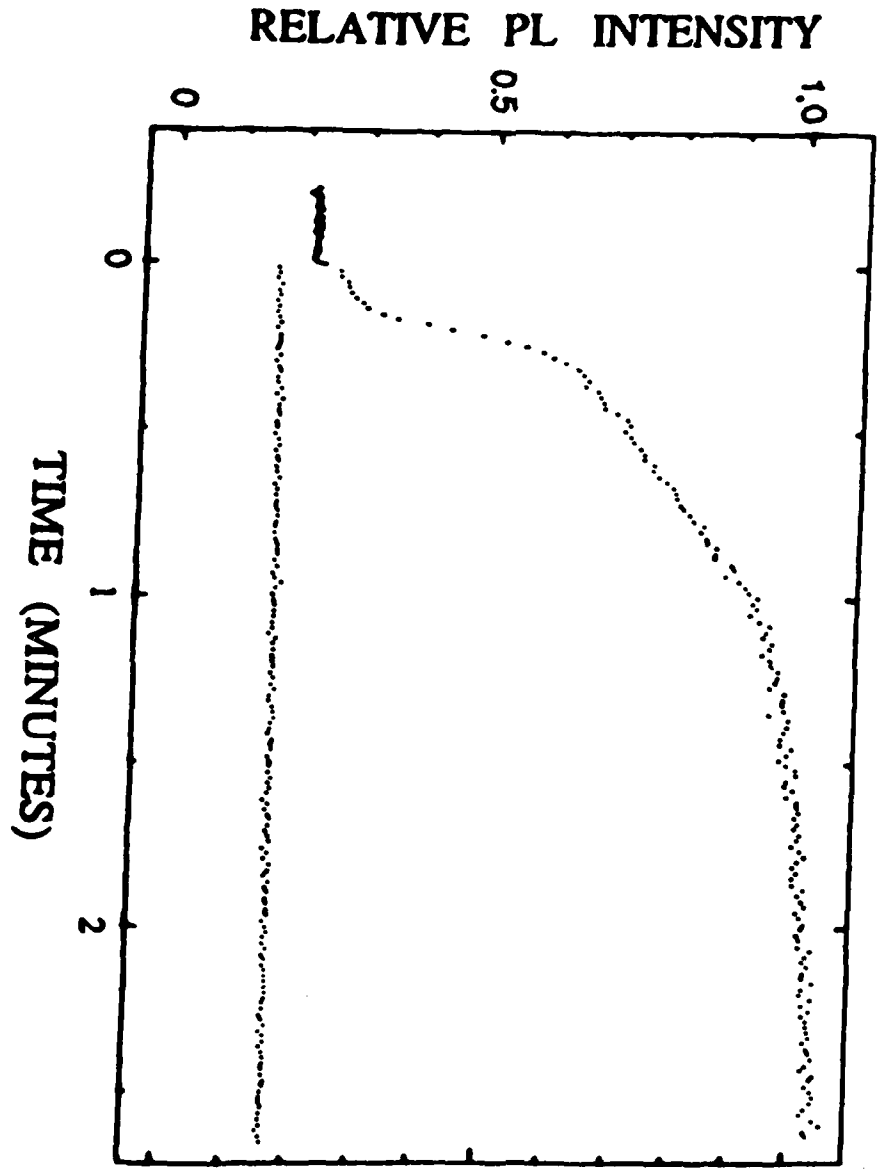
RELATIVE PL INTENSITY
0
0.5
1.0
TIME (MINUTES)
0
1
2

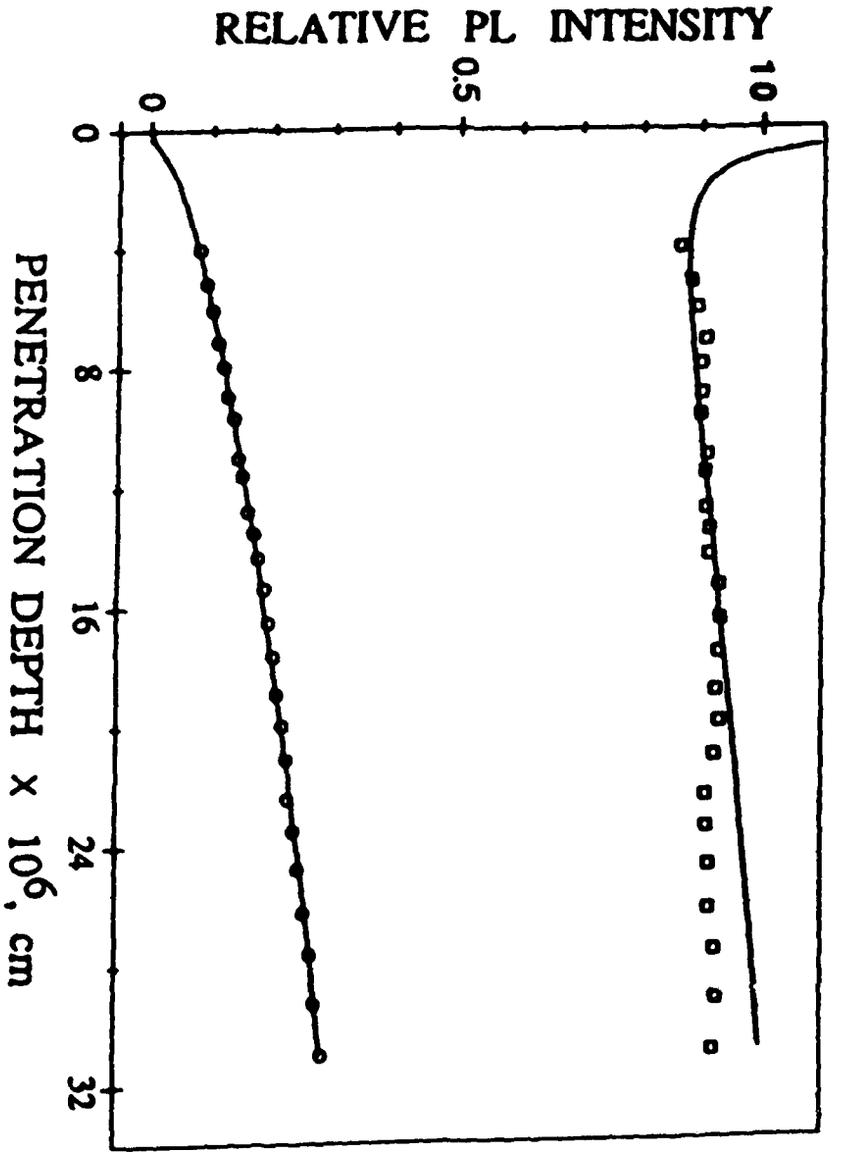
RELATIVE PL INTENSITY
0
0.5
10
PENETRATION DEPTH x 10^6, cm
0
8
16
24
32

END

9-87

DTIC